

---

# LEARNING SPIKING NEURAL SYSTEMS WITH THE EVENT-DRIVEN FORWARD-FORWARD PROCESS

---

Alexander Ororbia

Rochester Institute of Technology  
ago@cs.rit.edu

## ABSTRACT

We develop a novel credit assignment algorithm for information processing with spiking neurons without requiring feedback synapses. Specifically, we propose an event-driven generalization of the forward-forward and the predictive forward-forward learning processes for a spiking neural system that iteratively processes sensory input over a stimulus window. As a result, the recurrent circuit computes the membrane potential of each neuron in each layer as a function of local bottom-up, top-down, and lateral signals, facilitating a dynamic, layer-wise parallel form of neural computation. Unlike spiking neural coding, which relies on feedback synapses to adjust neural electrical activity, our model operates purely online and forward in time, offering a promising way to learn distributed representations of sensory data patterns with temporal spike signals. Notably, our experimental results on several pattern datasets demonstrate that the even-driven forward-forward (ED-FF) framework works well for training a dynamic recurrent spiking system capable of both classification and reconstruction.

**Keywords** Forward learning · Brain-inspired computing · Spiking neural networks

## 1 Introduction

The idea of “mortal computation” [25] challenges one of the foundational principles upon which general purpose computers have been built. Specifically, computation, as it is conducted today, is driven by the strong separation of software from hardware, i.e., this means that the knowledge contained within a program written in the software is “immortal”, allowing it to be copied to different physical copies of the hardware itself. Machine learning models and algorithms, which can be viewed as programs that adjust themselves in accordance with data, also rely upon this separation. Mortal computation, in contrast, means that once the hardware medium fails or “dies”, the knowledge encoded within it will also “die” or disappear, much akin to what would happen to the knowledge acquired by a biological organism when it is no longer able to maintain homeostasis. Despite the seeming disadvantage that comes with tightly bounding the software’s fate with that of the hardware it is implemented within, abandoning the immortal nature of computation brings with it the important promise of substantial savings in energy usage as well as a reduction in the cost of creating the hardware needed to execute the required computations. Working towards mortal computation addresses some of the concerns and questions that have recently emerged in artificial intelligence (AI) research [1, 4, 75, 69, 61]: how may we design intelligent systems that do not escalate computational and carbon costs? In essence, there is a strong motivation to move away from *Red AI*, which is driven by the dominance of immortal computation, towards *Green AI* [69], which mortal computation would naturally facilitate.

As was further argued in [54], moving towards mortal computation would also likely entail challenging another important separation made in deep learning – the separation between inference and credit assignment. Specifically, in deep neural networks, including the more recent neural transformers [11, 16, 5] that drive large language models (typically pre-trained on gigantic text databases), are fit to training datasets in such a way that learning, carried out via the backpropagation of errors (backprop) algorithm [64], is treated as a separate computation distinct from the mechanisms in which information is propagated through the network itself. In contrast, an adaptive system that could take advantage of mortal computing will most likely need to engage in *intertwined inference-and-learning* [60, 58, 55, 53], the framing that neurobiological learning and inference in the brain are not really two completely

distinct, separate processes but rather complementary ones that depend on one another, the formulations of which are motivated and integrated with the properties of the underlying neural circuitry (and the hardware that instantiates it) in mind. Neural systems, in this context, would adapt to external information based on the properties of the hardware that they run on, governed by homeostatic-like constraints. From this perspective, it would be beneficial for research in brain-inspired credit assignment to look to computational frameworks that embody intertwined inference-and-learning; important candidate frameworks include predictive processing/coding [62, 18, 72, 53, 66], contrastive Hebbian learning [45, 48, 68], and forward-only learning [32, 25, 54, 31], each with their own strengths and weaknesses. This direction could prove invaluable for AI research, providing not only another important link between cognitive science, computational neuroscience, and machine learning, but also a critical means of running neural systems composed of trillions of synapses (as in the brain), while only consuming a few watts of energy.

Among the potential forms of hardware that could embody mortal computation and intertwined inference-and-learning, e.g., memristors [27, 76], liquid crystal spatial light modulators [6, 13], Field Programmable Gate Arrays (FPGAs) [34, 47], neuromorphic chips [19, 63] have emerged as one promising candidate. Neuromorphic platforms offer an incredibly efficient, low-energy means of conducting numerical calculations, facilitating resource-constrained edge computation [33, 9]. Spiking neural networks (SNNs), sometimes branded as the third generation of neural networks [38, 40, 39, 14, 15], are a particular type of brain-inspired adaptive system and are naturally suited for implementation in neuromorphic hardware. Properly exploiting the design and properties of such chips enables the crafting model and algorithmic designs that embody mortal computation. However, developing effective, stable processes for conducting credit assignment in SNNs remains a challenge, particularly if the synaptic adjustment process is to rely on the properties of the discretely spiking neural units that compose them. One of the most promising directions for facilitating dynamic learning in complex SNNs is to generalize intertwined inference-and-learning credit assignment, such as predictive coding [50], at the spike train level. Important qualities that should characterize the computations of such systems would include: **1)** no requirement for differentiability in the spike-based communication (as backprop through time applied to SNNs requires the design of surrogate functions [43, 79]), **2)** no forward-locking [29] in the information propagation (a layer of neurons can compute their activity values without waiting on other layers to update their own), **3)** no backward-locking [29] in the synaptic update phase (adjustments to synapses for one layer of neurons can be executed in parallel with other layers across time – updates are local in both space and time), and **4)** no feedback synaptic pathways are fundamentally required to calculate synaptic change.

In this work, we satisfy the above criterion by developing a novel formulation of forward-only learning [32], specifically the forward-forward (FF) [25] and predictive forward-forward (PFF) [54] learning algorithms, for the case of systems that center around spike-based communication. Our core contributions in this study include: **1)** the design of a recurrent spiking neural network that fundamentally exhibits layer-wise parallelism, driven by a top-down, bottom-up, and lateral set of pressures that do not require feedback synaptic pathways, **2)** the event-driven forward-forward (ED-FF) credit assignment process for locally adapting the synapses of spiking neural systems in an online, dynamic fashion, potentially serving as a process that could complement spike-timing dependent plasticity (STDP) [3], **3)** a simple and fast mechanism for learning a spike-based classifier without resorting to the expensive energy-based classification scheme that characterizes FF and PFF-based systems, and **4)** a quantitative evaluation of the classification generalization ability of our spiking system learned with ED-FF.

## 2 Learning Spiking Networks with Event-Driven Forward-Forward Adjustment

**Notation** We use  $\odot$  to indicate the Hadamard product (or element-wise multiplication) and  $\cdot$  to denote a matrix/vector multiplication.  $(\mathbf{v})^T$  is the transpose of  $\mathbf{v}$ . Matrices/vectors are depicted in bold font, e.g., matrix  $\mathbf{M}$  or vector  $\mathbf{v}$  (scalars shown in italic).  $\mathbf{z}_j$  will refer to extracting  $j$ th scalar from vector  $\mathbf{z}$ .<sup>1</sup> Finally,  $\|\mathbf{v}\|_2$  denotes the Euclidean norm of vector  $\mathbf{v}$ . A sensory input pattern has shape  $\mathbf{x} \in \mathcal{R}^{J_0 \times 1}$  ( $J_0$  is the number of input features, e.g., pixels), a label vector has shape  $\mathbf{y} \in \mathcal{R}^{C \times 1}$  (where  $C$  is the number of classes), and any layer inside a neural system has shape  $\mathbf{z}^\ell \in \mathcal{R}^{J_\ell \times 1}$  -  $J_\ell$  is the number of neurons in layer  $\ell$ .

### 2.1 The Recurrent Spiking Neural Circuit Dynamics

The neural system that we will design and study is composed of recurrent layers that operate in parallel with each other, i.e., at time  $t$  each layer  $\ell$  made up of  $J_\ell$  neurons will take in as input the previous (spike) signals emitted (at time  $t - 1$ ) from the neurons immediately below (from layer  $\ell - 1$ ) and immediately above (from layer  $\ell + 1$ ). , which will prove useful to encourage neural units to form spike representations that encode discriminative information. Finally, the neurons in each of these layers will be laterally connected to each other, where the

<sup>1</sup>Note that, in some cases, extra subscript tags will appear, such as in  $\mathbf{z}_{tag,j}$ , which means extract the  $j$ th element of  $\mathbf{z}_{tag}$ .

synapses that relate them will enforce a form of cross-inhibition, i.e., neurons that more strongly active will suppress the activities of others (resulting in an emergent form of  $K$  winners-take-all competition, where  $K$  is dynamic and variable).

Formally, the overall model, composed of  $L$  layers of neural processing elements, is fully parameterized by the construct  $\Theta = \{\mathbf{W}^1, \mathbf{V}^1, \mathbf{M}^1, \mathbf{B}^1, \dots, \mathbf{W}^\ell, \mathbf{V}^\ell, \mathbf{M}^\ell, \mathbf{B}^\ell, \dots, \mathbf{W}^L, \mathbf{M}^L, \mathbf{B}^L\}$  (note that the top layer  $L$  does not contain any top-down recurrent synapses as there would be no layer above  $L$ ) where, as described earlier, each layer's stateful activation is driven by bottom-up synaptic connections (inside of matrix  $\mathbf{W}^\ell \in [-1, 1]^{J_\ell \times J_{\ell-1}}$ ), top-down mediating synapses (inside of matrix  $\mathbf{V}^\ell \in [-1, 1]^{J_\ell \times J_{\ell+1}}$ ), lateral inhibition synapses (inside of matrix  $\mathbf{M}^\ell \in [0, 1]^{J_\ell \times J_\ell}$ ), and context-mediating synapses (inside of matrix  $\mathbf{B}^\ell \in [-1, 1]^{J_\ell \times C}$ ). Note that all of the constituent matrices contain values that are bounded between  $-1$  and  $1$ , except for  $\mathbf{M}^\ell$  which only contains positive values in the range of  $[0, 1]$ . The dynamics of any given layer  $\ell$  in our recurrent spiking system follow that of a leaky integrator and are concretely calculated as follows:

$$\mathbf{j}^\ell(t) = \mathbf{W}^\ell \cdot \mathbf{s}^{\ell-1}(t) + \mathbf{V}^\ell \cdot \mathbf{s}^{\ell+1}(t) - (\mathbf{M}^\ell \odot (1 - \mathbf{I}^\ell)) \cdot \mathbf{s}^\ell(t) + \mathbf{B}^\ell \cdot \mathbf{s}_y(t) \quad (1)$$

$$\mathbf{v}^\ell(t + \Delta t) = \mathbf{v}^\ell(t) + \frac{\Delta t}{\tau_m} \left( -\mathbf{v}^\ell(t) + R_m \mathbf{j}^\ell(t) \right) \quad (2)$$

$$\mathbf{s}^\ell(t) = \mathbf{v}^\ell(t + \Delta t) > v_{thr}^\ell, \text{ and, } \mathbf{v}^\ell(t) = \mathbf{v}^\ell(t + \Delta t) \odot (1 - \mathbf{s}^\ell(t)) \quad (3)$$

$$v_{thr}^\ell = v_{thr}^\ell + \lambda_v \left( \left( \sum_{j=1}^{J_\ell} \mathbf{s}^\ell(t)_j \right) - 1 \right) \quad (4)$$

where  $\mathbf{j}^\ell(t)$  is the vector containing the electrical current input to each neural cell in layer  $\ell$ ,  $\mathbf{v}^\ell(t)$  is the vector containing the current membrane potential (voltage) values for each cell in layer  $\ell$ , and  $\mathbf{s}^\ell(t)$  is the vector containing each cell's binary spike output in layer  $\ell$ .  $R_m$  is the resistance constant, (deci)Ohms, for layer  $\ell$ ,  $\Delta t$  is the integration time constant on the order of milliseconds (ms), and  $\tau_m$  is the membrane time constant (in ms). In the bottom equation, we depolarize the membrane voltage back to a resting potential of 0 (deci)volts through binary gating and do not consider modeling a refractory period (we omit both relative and absolute refractory periods for simplicity). Notice in Equation 4, we simulate a simple adaptive threshold  $v_{thr}^\ell \in [0, \infty)$  (further constrained to be positive) which, at each time step  $t$ , either adds or subtracts a small value (scaled by  $\lambda_v$ , typically set to a number such as 0.001) to a layer's current threshold value based on how many spikes were recorded at time step  $t$  for layer  $\ell$ . Finally,  $\mathbf{s}^0(t)$  is the binary spike representation of the sensory input  $\mathbf{x}$  at time  $t$  and is created by sampling the normalized pixel values of  $\mathbf{x}$  (each dimension of  $\mathbf{x}$  is divided by the maximum pixel value 255), treating each dimension as Bernoulli probability.  $\mathbf{s}_y(t)$  is contextual spike train associated with  $\mathbf{x}$ , i.e., in this study,  $\mathbf{s}_y(t) = \mathbf{y}$  (it is clamped to the label during training).

One of the nice properties of the recurrent spiking system above is that it is layer-wise parallelizable and thus not forward-locked [29] (spike activities at any layer can be computed in parallel of the others) and, furthermore, not backward-locked (synaptic updates for any layer can be computed in parallel of the others). This stands in strong contrast to most (deep) SNN designs today, with some exceptions [50], given that many SNNs are typically feedforward, where each layer of spiking neurons depends on the spike activities of the layer that comes before them resulting in a forward-locked computation. Our spiking model ensures this important form of model-level parallelism by only enforcing leaky integrator spike activities to upon only immediately previously computed activities (of simulation step  $t - 1$ ).

## 2.2 Online Learning Dynamics

One key building block to our event-driven contrastive learning process is the trace variable. Specifically, in our recurrent spiking system above, we incorporate an additional compartment into each neural layer that is responsible for maintaining what is called an activity variable trace (or activation trace). Formally, this means that for each layer, a variable trace is dynamically updated as follows:

$$\mathbf{z}^\ell(t) = \mathbf{s}^\ell(t) - \frac{\Delta t}{\tau_{tr}} \mathbf{z}^\ell(t) \odot (1 - \mathbf{z}^\ell(t)) \quad (5)$$

where, in this work, the trace time constant was set to  $\tau_{tr} = 300$  ms. Importantly, an activation trace smooths out the sparse spike trains generated by the spiking model while still being biologically-plausible. Notably, a trace offers a dynamic rate-coded equivalent value that, in our neuronal layer model, is maintained within the actual neuronal cells likely in the form of the concentration of internal calcium ions [49], i.e., a variable trace could correspond to the glutamate bound to synaptic receptors. Desirably, this will allow our local adaptation rule to

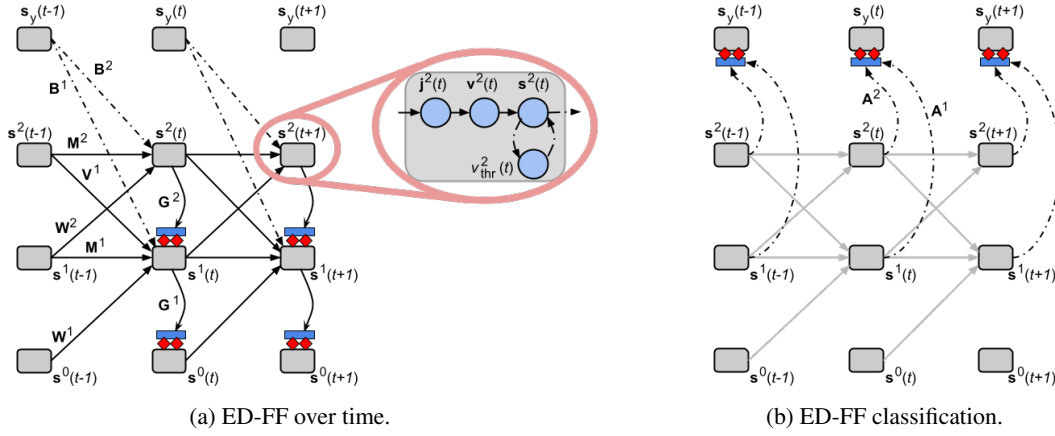


Figure 1: The ED-PFF learning process for our recurrent spiking network. (Left) The spiking network processes sensory spike train  $\{s^0(0), \dots, s^0(t), \dots, s^0(T)\}$ . The zoomed-in inset depicts, internally, that each activation layer is made up of at least four components, i.e., an electrical current model  $j^\ell(t)$ , a voltage model  $v^\ell(t)$ , a spike response function  $s^\ell(t)$ , and an adaptive threshold  $v_{thr}^\ell(t)$ . (Right) The same spiking network is shown predicting the context  $s_y(t)$  over time, where at each step  $t$ , the spiking classifier makes its current best guess  $\mu_y(t)$  of the context’s spike train and adjusts its relevant synapses using an error-driven Hebbian rule.

take place using spike information, bringing it closer to STDP-like learning, rather than being used directly on the voltage or electrical current values, like in other related efforts [31].<sup>2</sup>

Given the activation trace above, we can now formulate the objective that each layer of our spiking system will try to optimize at each step of simulated time. Specifically, in our synaptic adjustment process, *event-driven forward-forward (ED-FF) learning*, we propose adjusting the synaptic strengths in the recurrent spiking model above through a generalization of the goodness principle inherent to forward-forward [25] and predictive forward-forward [54] learning rules to the case of spiking neurons. As a result, the cost function takes the following form<sup>3</sup>:

$$\mathcal{L}_G(\mathbf{z}^\ell(t), y_{type}) = -\frac{1}{N} \sum_{i=1}^N y_{type} \log p(y_{type} = 1)_\ell + (1 - y_{type}) \log p(y_{type} = 0)_\ell, \quad (6)$$

$$\text{where } p(y_{type} = 1)_\ell = \frac{1}{1 + \exp(-(\sum_{j=1}^{J_\ell} (\mathbf{z}_j^\ell(t))^2 - \theta_z))} \quad (7)$$

where  $y_{type} \in \{0, 1\}$  is an integer that denotes the current sensory input’s “type”, i.e., 1 indicates that the current  $(\mathbf{x}, \mathbf{y})$  is a positive sensory input while 0 indicates that it is a negative sensory input.  $\theta_z$  is a threshold for comparing the square of the trace activity values against, set to  $\theta_z = 6.5$  in this paper. Given the above local cost function, each synaptic matrix in one layer of the system may now be adjusted with a Hebbian-like rule as follows:

$$\delta^\ell(t) = 2 \frac{\partial \mathcal{L}_G(\mathbf{z}^\ell(t), y_{type})}{\partial \sum_j^{J_\ell} (\mathbf{z}_j^\ell(t))^2} \quad (8)$$

$$\Delta \mathbf{W}^\ell = (R_m \delta^\ell(t) \cdot (\mathbf{s}^{\ell-1}(t-1))^T) + \lambda_d (\mathbf{s}^\ell(t) \cdot (1 - \mathbf{s}^{\ell-1}(t))^T) \quad (9)$$

$$\Delta \mathbf{V}^\ell = (R_m \delta^\ell(t) \cdot (\mathbf{s}^{\ell+1}(t-1))^T) + \lambda_d (\mathbf{s}^\ell(t) \cdot (1 - \mathbf{s}^{\ell+1}(t))^T) \quad (10)$$

$$\Delta \mathbf{M}^\ell = (R_m \delta^\ell(t) \cdot (\mathbf{s}^\ell(t-1))^T) + \lambda_d (\mathbf{s}^\ell(t) \cdot (1 - \mathbf{s}^\ell(t))^T) \quad (11)$$

$$\Delta \mathbf{B}^\ell = (R_m \delta^\ell(t) \cdot (\mathbf{s}_y(t-1))^T) + \lambda_d (\mathbf{s}^\ell(t) \cdot (1 - \mathbf{s}_y(t))^T) \quad (12)$$

where  $\lambda_d = 0.00005$  is the synaptic decay factor. Notice that the update to each of the four key synaptic matrices which characterize the computation of layer  $\ell$  depends on the easily computed partial derivative  $\delta^\ell(t)$  of the local

<sup>2</sup>We did implement an alternative form of ED-FF using a gated voltage rule, as noted later in this paper, but found that the trace-based rule yielded the best overall performance with respect to classification.

<sup>3</sup>An alternative form to the trace-based rule we used in this study simply replaces the left argument of the local loss function as follows:  $\mathcal{L}_G(\mathbf{v}^\ell(t) \odot \mathbf{s}^\ell(t), y_{type})$ . This is what we refer to as the “gated voltage rule” which has the advantage of no longer requiring the tracking of a spike activity trace, i.e., it only requires the use of the spike vector at  $t$  as a binary multiplicative gate against the current voltage values. However, we found that, in preliminary experiments, that this rule slightly, albeit consistently, underperformed the trace-based form of the loss and we thus do not investigate it further.

contrastive function  $\mathcal{L}_G(\mathbf{z}^\ell(t), y_{type})$ . We postulate that, biologically,  $\delta^\ell(t)$  (scaled by the resistance  $R_m$ ) would be implemented either in the form of a (neurotransmitter) chemical signal or alternatively as a separate population of neural units that encode this signal (much akin to the error neurons that characterize predictive processing [8]).

Finally, to fully emulate the predictive forward-forward (PFF) adaptation process (and thus incorporate its reconstruction/generative potential), we introduce an additional set of matrices containing the generative synapses – this means that we extend our model parameters to  $\Theta \cup \Theta_g$  where  $\Theta_g = \{\mathbf{G}^1, \dots, \mathbf{G}^\ell, \dots, \mathbf{G}^L\}$ . Desirably, each synaptic matrix  $\mathbf{G}^\ell$  is directly wired to each layer  $\ell$ , forming a local prediction of the activity of  $\mathbf{s}^\ell(t)$  as follows:

$$\mathbf{v}_\mu^\ell(t + \Delta t) = \mathbf{v}_\mu^\ell(t) + \frac{\Delta t}{\tau_m} \left( -\mathbf{v}_\mu^\ell(t) + R_m(\mathbf{G}^{\ell+1} \cdot \mathbf{s}^{\ell+1}(t)) \right) \quad (13)$$

$$\mathbf{s}_\mu^\ell(t) = \mathbf{v}_\mu^\ell(t + \Delta t) > v_{thr, \mu}, \quad \mathbf{v}_\mu^\ell(t) = \mathbf{v}_\mu^\ell(t + \Delta t) \odot (1 - \mathbf{s}_\mu^\ell(t)) \quad (14)$$

$$\mathbf{e}^\ell(t) = \mathbf{s}_\mu^\ell(t) - \mathbf{s}^\ell(t) \quad (15)$$

$$v_{thr, \mu}^\ell = v_{thr, \mu}^\ell + \lambda_v \left( \left( \sum_{j=1}^{J_\ell} \mathbf{s}_{\mu, j}^\ell(t) \right) - 1 \right) \quad (16)$$

where we observe that error mismatch units  $\mathbf{e}^\ell(t)$  have been introduced that specialize in tracking the disparity between prediction spike  $\mathbf{s}_\mu^\ell(t)$  and spike representation  $\mathbf{s}^\ell(t)$ . To update each generative matrix  $\mathbf{G}^\ell$ , we may then use the simple Hebbian update rule:

$$\Delta \mathbf{G}^\ell = (R_m \mathbf{e}^{\ell-1}(t)) \cdot (\mathbf{s}^\ell(t))^T. \quad (17)$$

When making local predictions and calculating mismatches as above, the full energy-like objective, at time  $t$ , of our spiking neural system becomes:

$$\mathcal{L}(t, \Theta) = \sum_{\ell=0}^L \begin{cases} \mathcal{L}_G(\mathbf{z}^\ell(t), y_{type}) & \text{if } \ell = L \\ \frac{1}{2} \|\mathbf{s}_\mu^\ell(t) - \mathbf{s}^\ell(t)\|_2^2 & \text{if } \ell = 0 \\ \mathcal{L}_G(\mathbf{z}^\ell(t), y_{type}) + \frac{1}{2} \|\mathbf{s}_\mu^\ell(t) - \mathbf{s}^\ell(t)\|_2^2 & \text{otherwise.} \end{cases} \quad (18)$$

Notice that each layer of the system is maximizing its goodness while further learning a (temporal) mapping between its own spike train to the one of the layer below it (i.e., a mapping that minimizes a measurement of local predictive spike error). The mismatch units we model explicitly in Equation 15 directly follows from taking the partial derivative of the local objective in Equation 18 with respect to  $\mathbf{s}_\mu^\ell(t)$ . Finally, across a full stimulus window of length  $T$ , the spiking system would be globally optimizing the following sequence loss:

$$\mathcal{L}(\Theta) = \sum_{t=1}^T \mathcal{L}(t, \Theta). \quad (19)$$

In effect, the spiking neural system that we simulate in this work attempts to incrementally optimize the sequence loss above when processing a data sample  $(\mathbf{x}, \mathbf{y})$ , conducting a form of online adaptation by computing synaptic adjustments given the current state of  $\Theta$  at simulation step  $t$ .

### 2.3 Spike-Driven Classification and its Fast Approximation

To perform classification with the recurrent spiking system model described in the previous few sections, one must run a scheme similar to [25, 54] where one iterates over all possible class values, i.e., setting the context  $\mathbf{y}$  equal to the one-hot encoding of class  $c \in \{1, 2, \dots, C\}$ . Specifically, for each class index  $c$ , we encode sensory input  $\mathbf{x}$  and its possible context  $\mathbf{y}_c = \mathbf{1}_c$ <sup>4</sup> into the system over a stimulus window of  $T$  steps and record the goodness summed across layers, averaged over time, i.e.,  $\mathcal{G}_{y=c} = \frac{1}{T} \sum_{t=1}^T \sum_{\ell=1}^L \sum_{j=1}^{J_\ell} (\mathbf{z}_j^\ell(t))^2$ . This time-averaged goodness value is computed for all class indices  $y = 1, 2, \dots, C$ , resulting in an array of  $C$  goodness scores, i.e.,  $G = \{\mathcal{G}_{y=1}, \mathcal{G}_{y=2}, \dots, \mathcal{G}_{y=C}\}$ . The argmax operation is applied to this array  $G$  to obtain the index of the class with the highest average goodness value, i.e.,  $c_{pred} = \operatorname{argmax}_{c \in C} G$ .

While the above per-class class process would work fine for reasonable values of  $C$ , it would not scale well to a high number of classes (i.e., very large values of  $C$ ) as the above process requires simulating the spiking network over  $C$  stimulus windows in order to compute a predicted label index that corresponds to maximum goodness. However, we found that one could avoid conducting this classification process entirely if a spiking classification output layer is incorporated into our recurrent spiking system. This classifier, which takes in as input the spike output of each layer of our recurrent system, is jointly learned with the rest of the model parameters and entails extending  $\Theta$  one more time so that it includes classification-specific synapses, i.e.,  $\Theta \cup \Theta_c$  where  $\Theta_c = \{\mathbf{A}^1, \dots, \mathbf{A}^\ell, \dots, \mathbf{A}^L\}$ .

<sup>4</sup> $\mathbf{1}_c$  is the indicator function, which returns one if the index  $i$  in  $\mathbf{y}$  is equal to the desired class index  $c \in \{1, 2, \dots, C\}$ .

**Algorithm 1** The event-driven (predictive) forward-forward credit assignment algorithm.

---

```

1: Input: sample  $(\mathbf{y}, \mathbf{x})$ , data label  $y_{type}$  (binary label: 1 = "positive", 0 = "negative"), SNN parameters  $\Theta$ 
2: Hyperparameters: SGD step size  $\eta$ , stimulus time  $T$ , integration constant  $\Delta t$ , time constants  $\tau_m$  and  $\tau_{tr}$ ,
3: adaptive threshold step  $\lambda_v$ 
4:  $// \leftarrow$  denotes the overriding of a variable/object,  $\Omega()$  is a bounding function
5: function SIMULATE( $(\mathbf{y}, \mathbf{x}, y_{type}), \Theta$ )
6:   for  $t = 1$  to  $T$  do
7:      $\mathbf{s}^0(t) \sim \mathcal{B}(1, p = \mathbf{x})$   $\triangleright$  Sample sensory input to get an input spike at time  $t$ 
8:     for  $\ell = 1$  to  $L$  do
9:        $//$  Compute the current and voltage components of layer  $\ell$ 
10:      if  $\ell < L$  then
11:         $\mathbf{j}^\ell(t) = \mathbf{W}^\ell \cdot \mathbf{s}^{\ell-1}(t) + \mathbf{V}^\ell \cdot \mathbf{s}^{\ell+1}(t) - (\mathbf{M}^\ell \odot (1 - \mathbf{I}^\ell)) \cdot \mathbf{s}^\ell(t) + \mathbf{B}^\ell \cdot \mathbf{s}_y(t)$ 
12:      else
13:         $\mathbf{j}^\ell(t) = \mathbf{W}^\ell \cdot \mathbf{s}^{\ell-1}(t) - (\mathbf{M}^\ell \odot (1 - \mathbf{I}^\ell)) \cdot \mathbf{s}^\ell(t) + \mathbf{B}^\ell \cdot \mathbf{s}_y(t)$ 
14:         $\mathbf{v}^\ell(t + \Delta t) = \mathbf{v}^\ell(t) + \frac{\Delta t}{\tau_m} \left( -\mathbf{v}^\ell(t) + R_m \mathbf{j}^\ell(t) \right)$ 
15:         $//$  Run the spike model given  $\mathbf{j}(t)$  and  $\mathbf{v}(t)$  (and depolarize  $\mathbf{v}(t)$  if applicable)
16:         $\mathbf{s}^\ell(t) = \mathbf{v}^\ell(t + \Delta t) > v_{thr}^\ell, \mathbf{v}^\ell(t) = \mathbf{v}^\ell(t + \Delta t) \odot (1 - \mathbf{s}^\ell(t)), v_{thr}^\ell = v_{thr}^\ell + \lambda_v ((\sum_{j=1}^{J_\ell} \mathbf{s}^\ell(t)_j) - 1)$ 
17:         $//$  Update the activation trace for layer  $\ell$ 
18:         $\mathbf{z}_t^\ell = \mathbf{s}_t^\ell - \frac{\Delta t}{\tau_{tr}} \mathbf{z}_t^\ell \odot (1 - \mathbf{z}_t^\ell)$ 
19:         $//$  Calculate local synaptic adjustments and update its synaptic efficacies
20:        Get loss  $\mathcal{L}_G(\mathbf{z}^\ell(t), y_{type})$  (Equation 6) & its partial derivative w.r.t.  $\mathbf{z}^\ell(t)$ , i.e.,  $\delta^\ell(t) = 2 \frac{\partial \mathcal{L}_G(\mathbf{z}^\ell(t), y_{type})}{\partial \sum_j \mathbf{z}_j^\ell(t)}$ 
21:         $\Delta \mathbf{W}^\ell = (R_m \delta^\ell(t) \cdot (\mathbf{s}^{\ell-1}(t-1))^T) + \lambda_d (\mathbf{s}^\ell(t) \cdot (1 - \mathbf{s}^{\ell-1}(t))^T), \mathbf{W}^\ell \leftarrow \Omega(\mathbf{W}^\ell - \eta \Delta \mathbf{W}^\ell)$ 
22:         $\Delta \mathbf{V}^\ell = (R_m \delta^\ell(t) \cdot (\mathbf{s}^{\ell+1}(t-1))^T) + \lambda_d (\mathbf{s}^\ell(t) \cdot (1 - \mathbf{s}^{\ell+1}(t))^T), \mathbf{V}^\ell \leftarrow \Omega(\mathbf{V}^\ell - \eta \Delta \mathbf{V}^\ell)$ 
23:         $\Delta \mathbf{M}^\ell = (R_m \delta^\ell(t) \cdot (\mathbf{s}^\ell(t-1))^T) + \lambda_d (\mathbf{s}^\ell(t) \cdot (1 - \mathbf{s}^\ell(t))^T), \mathbf{M}^\ell \leftarrow \Omega(\mathbf{M}^\ell - \eta \Delta \mathbf{M}^\ell)$ 
24:         $\Delta \mathbf{B}^\ell = (R_m \delta^\ell(t) \cdot (\mathbf{s}_y(t-1))^T) + \lambda_d (\mathbf{s}^\ell(t) \cdot (1 - \mathbf{s}_y(t))^T), \mathbf{B}^\ell \leftarrow \Omega(\mathbf{B}^\ell - \eta \Delta \mathbf{B}^\ell)$ 
25:         $//$  Run  $\ell$ th local predictor, error neurons and adjust its synaptic efficacies
26:         $\mathbf{v}_\mu^\ell(t + \Delta t) = \mathbf{v}_\mu^\ell(t) + \frac{\Delta t}{\tau_m} \left( -\mathbf{v}_\mu^\ell(t) + R_m (\mathbf{G}^{\ell+1} \cdot \mathbf{s}^{\ell+1}(t)) \right)$ 
27:         $\mathbf{s}_\mu^\ell(t) = \mathbf{v}_\mu^\ell(t + \Delta t) > v_{thr, \mu}^\ell, \mathbf{v}_\mu^\ell(t) = \mathbf{v}_\mu^\ell(t + \Delta t) \odot (1 - \mathbf{s}_\mu^\ell(t)), v_{thr, \mu}^\ell = v_{thr, \mu}^\ell + \lambda_v ((\sum_{j=1}^{J_\ell} \mathbf{s}_{\mu, j}^\ell(t)) - 1)$ 
28:         $\mathbf{e}^\ell(t) = \mathbf{s}_\mu^\ell(t) - \mathbf{s}^\ell(t)$   $\triangleright$  Calculate the error/mismatch activities
29:         $\Delta \mathbf{G}^\ell = (R_m \mathbf{e}^{\ell-1}(t)) \cdot (\mathbf{s}^\ell(t))^T, \mathbf{G}^\ell \leftarrow \Omega(\mathbf{G}^\ell - \eta \Delta \mathbf{G}^\ell)$ 
30:         $//$  Calculate classifier outputs and adjust its synaptic efficacies
31:         $\mathbf{v}_y(t + \Delta t) = \mathbf{v}_y(t) + \frac{\Delta t}{\tau_m} \left( -\mathbf{v}_y(t) + R_m (\sum_{\ell=1}^L \mathbf{A}^\ell \cdot \mathbf{s}^\ell(t)) \right)$ 
32:         $\mu_y(t) = \mathbf{v}_y(t + \Delta t) > v_{thr}^y, \mathbf{v}_y(t) = \mathbf{v}_y(t + \Delta t) \odot (1 - \mu_y(t)), v_{thr}^y = v_{thr}^y + \lambda_v ((\sum_{j=1}^C \mu_{y, j}(t)) - 1)$ 
33:         $\Delta \mathbf{A}^\ell = (\mu_y(t) - \mathbf{s}_y(t)) \cdot (\mathbf{s}^\ell(t))^T, \mathbf{A}^\ell \leftarrow \Omega(\mathbf{A}^\ell - \eta \Delta \mathbf{A}^\ell), \forall \ell = 1 \dots L$ 
34:   Return  $\Theta = \{\mathbf{W}^\ell, \mathbf{V}^\ell, \mathbf{M}^\ell, \mathbf{B}^\ell\}_{\ell=1}^L \cup \{\mathbf{G}^\ell\}_{\ell=1}^L \cup \{\mathbf{A}^\ell\}_{\ell=1}^L$   $\triangleright$  Output newly updated model parameters

```

---

Concretely, the classifier module operates according to the following dynamics:

$$\mathbf{v}_y(t + \Delta t) = \mathbf{v}_y(t) + \frac{\Delta t}{\tau_m} \left( -\mathbf{v}_y(t) + R_m \left( \sum_{\ell=1}^L \mathbf{A}^\ell \cdot \mathbf{s}^\ell(t) \right) \right) \quad (20)$$

$$\mu_y(t) = \mathbf{v}_y(t + \Delta t) > v_{thr}^y, \mathbf{v}_y(t) = \mathbf{v}_y(t + \Delta t) \odot (1 - \mu_y(t)) \quad (21)$$

$$v_{thr}^y = v_{thr}^y + \lambda_v \left( \left( \sum_{j=1}^C \mu_{y, j}(t) \right) - 1 \right) \quad (22)$$

where we notice that the contextual prediction voltage  $\mathbf{v}_y(t)$  is the result of aggregating across the spike vector messages transmitted from layers  $\ell = 1$  to  $\ell = L$  (as in Equation 20). Each synaptic matrix  $\mathbf{A}^\ell$  of the spiking classifier is adjusted according to the following Hebbian rule:

$$\Delta \mathbf{A}^\ell = (\mu_y(t) - \mathbf{s}_y(t)) \cdot (\mathbf{s}^\ell(t))^T. \quad (23)$$

If the additional synaptic classification parameters are learned, then, at test time (when synaptic adjustment is disabled/turned off), one can simply provide the spiking system with the sensory input  $\mathbf{x}$  with no context  $\mathbf{y}$  and obtain an estimated context output  $\bar{\mathbf{y}}$ . This  $\bar{\mathbf{y}}$  is a function of the system's predictions/outputs across time, i.e., it is the approximate output/label distribution  $\bar{\mathbf{y}} = \exp(\sum_{t=1}^T \mu_y(t)) / \sum_{c=1}^C \exp(\sum_{t=1}^T \mu_{y, c}(t))_c$ . Note that the conditional log likelihood  $\log p(\mathbf{y}|\mathbf{x}; \Theta)$  of the spiking model can now be measured using this approximate label probability distribution. Although learning this spiking classifier entails a memory cost of up to  $L$  additional

Table 1: Measurements of generalization error of spiking networks trained with different credit assignment processes. “Imp.” denotes implementation. BP-FFN is the rate-coded comparison model (a backprop-trained feedforward neural network).

	MNIST	K-MNIST
BP-FFN	$1.300 \pm 0.023$	$6.340 \pm 0.202$
Spiking-RBM [42]	11.000	—
SNN-LM [22]	5.930	—
Power-Law STDP [12]	5.000	—
DRTP (Imp.)	$6.451 \pm 0.172$	$21.320 \pm 0.130$
L2-SigProp (Imp.)	$11.425 \pm 0.0152$	$35.045 \pm 0.005$
BFA (Imp.)	$3.352 \pm 0.102$	$11.250 \pm 0.050$
SigProp (Imp.)	$6.240 \pm 0.030$	$24.820 \pm 0.200$
ED-FF (Ours)	$2.540 \pm 0.030$	$8.860 \pm 0.021$

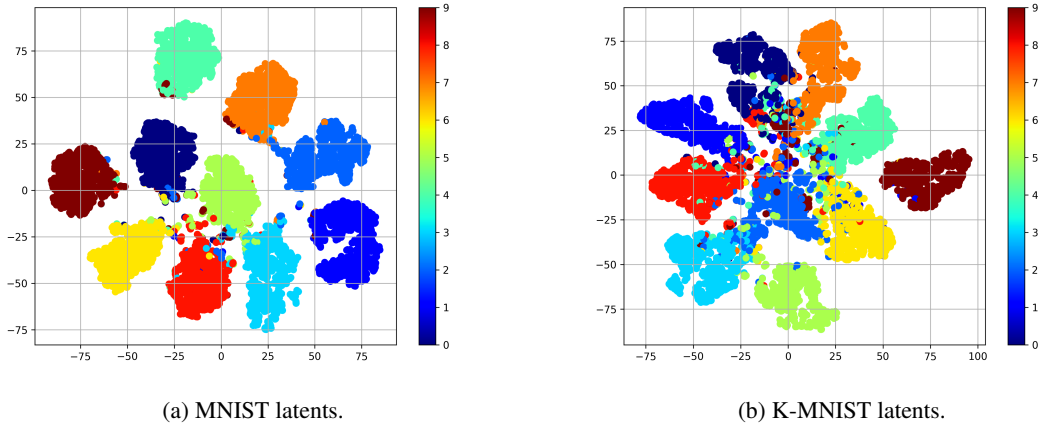


Figure 2: t-SNE visualizations of the latent space induced by recurrent spiking networks learned with the proposed event-driven forward-forward learning process. (Left) MNIST rate codes are visualized. (Right) K-MNIST rate codes are visualized.

synaptic matrices, the test-time inference of the spiking system will be significantly faster, thus making it suitable for on-chip computation.

In Algorithm 1, the processing and synaptic adjustment (via ED-FF) that our spiking system undergoes at time  $t$ , which includes the spiking classifier, is fully specified.

### 3 Experiments

#### 3.1 Experimental Setup

**Datasets:** The MNIST dataset [35] specifically contains images of handwritten digits across 10 different categories. Kuzushiji-MNIST (K-MNIST) is a challenging drop-in replacement for MNIST, containing images depicting hand-drawn Japanese Kanji characters [7] (each class corresponds to the character’s modern hiragana counterpart, with 10 total classes). For both datasets, image patterns are normalized to the range of  $[0, 1]$  by dividing pixel values by 255. The resulting pixel “probabilities” are then used to create sensory input spike trains by treating the normalized vector  $\mathbf{x}/255$  as the parameter vector for a multivariate Bernoulli distribution. The resulting distribution is then sampled at each time step  $t$  over the stimulus window of length  $T$ . Note that we do not preprocess the image data any further unlike other efforts related to spiking neural networks. However, we remark that it might be possible to obtain better performance by whitening image patterns (particularly in the case of natural images) or applying a transformation that mimics the result of neural encoding populations based on Gaussian receptive fields.

**Simulation Details:** We compare our proposed ED-FF process model with several comparable spiking network baselines: 1) a spiking network classifier trained with direct random target propagation (DTRP) [17], 2) a spiking network trained with broadcast feedback alignment (BFA) [67], 3) a spiking network trained with a simplified variant of signal propagation [32, 31] using a voltage-based rule and a local cost based on the Euclidean (L2) distance function (L2-SigProp), and 4) a spiking network trained using a simple generalization of local classifiers/errors (where each layer-wise classifier is learned jointly with the overall neural system) [44, 80]. Furthermore, we provide a rate-coded baseline model (i.e., one that does not operate with spike trains) represented by a tuned feedforward neural network trained by backprop (BP-FNN).

The network models simulated under each learning algorithm were designed to have two latent/hidden layers of 6400 leaky integrate-and-fire (LIF) neurons with connecting synaptic efficacies randomly initialized from a standard Gaussian distribution truncated to the range of  $[-1, 1]$  (except for the lateral synapses in ED-FF, which were truncated to  $[0, 1]$ ). All models further employed a spiking classifier of the same design (aggregating the spike vector outputs across all layers) as the one proposed for the ED-FF system in order a fair comparison (we found these hidden-to-output synapses improved generalization performance across the board).

Since all of the credit assignment algorithms, including our own, could support mini-batch calculations, we train all models with mini-batches of 200 patterns (randomly sampled without replacement from a training dataset) to speed up simulation and used the Adam adaptive learning rate [30] (with step size  $\eta = 0.002$ ) to physically adjust synaptic efficacies given the updates provided by any given algorithm. Each data point/batch  $(\mathbf{x}, \mathbf{y})$  was presented to all spiking networks for a stimulus window of  $T = 50$  steps (or 150 ms given  $\Delta t = 3$  ms). Finally, note that all spiking networks employed the same adaptive threshold update scheme that the ED-FF system used – it was observed that this mechanism improved training stability in all cases.

### 3.2 Benchmark Classification Results

In Table 1, we present our simulation results for our recurrent spiking model trained with event-driven forward-forward learning. Notice that, like many bio-physical spiking networks, even though we do not quite match the performance of backprop-based feedforward networks (essentially a purely rate-coded system), our generalization error comes surprisingly close. This is particularly promising given that the predicted context layer is a layer of spiking neurons itself. Furthermore, our ED-FF model comes the closest to matching the BP-FNN rate-coded baseline compared to the other SNN credit assignment algorithms. The BFA SNN comes in a close second place, illustrating that feedback synapses are still quite a powerful mechanism even though our goal was to demonstrate effective learning without feedback. We remark that our comparison does not include the spiking predictive coding model reported in [50], even though a slightly better generalization error was reported on MNIST. This model was not included given that is unsupervised and required post-fitting a log-linear classifier to rate code approximations of its top-most spike-train representations (and our focus in this study was on spiking models that jointly learned a spiking classifier with the internal representations of the sensory input).

In Figure 2, we examine the clusters that emerge within the latent space induced by a recurrent spiking network trained with ED-FF. To compute the latent vectors/codes, we form an approximate rate code from each data point’s resultant top-layer (layer  $s_t^3$ ) spike trains as follows:

$$\mathbf{c} = \frac{\gamma_c}{T} \sum_t \mathbf{s}_t^3 \quad (24)$$

with  $\gamma_c = 1$ . After feeding each data point  $\mathbf{x}$  (without its context  $\mathbf{y}$ ) in the test-set to our model and collecting its approximate top-layer rate-code vector  $\mathbf{c}$ , we visualize the emergent islands of rate codes using t-Distributed Stochastic Neighbor Embedding (t-SNE) [77]. Notice how, for both MNIST (Figure 2a) and K-MNIST (Figure 2b), clusters related to each category naturally form, qualitatively demonstrating why the ED-FF spiking model is able to classify unseen test patterns effectively. This is particularly impressive for K-MNIST, which is arguably the more difficult of the two datasets, which means that ED-FF adaptation is capable of extracting class-centric information from more complicated patterns.

Finally, in Figure 3, we examine the pattern reconstruction ability of our ED-FF spiking model on randomly sampled (without replacement) image patterns from the MNIST and K-MNIST databases. A single image reconstruction pattern  $\hat{\mathbf{x}}$  was created by computing an average across activation traces of the bottom-most predictor’s output spikes, collected during the  $T$ -length stimulus window as follows:

$$\hat{\mathbf{x}} = \frac{1}{T} \sum_{t=1}^T \mathbf{z}_\mu^0(t), \text{ where } \mathbf{z}_\mu^0(t) = \mathbf{s}_\mu^0(t) - \frac{\Delta t}{\tau_{tr}} \mathbf{z}_\mu^0(t) \odot (1 - \mathbf{z}_\mu^0(t)) \quad (25)$$

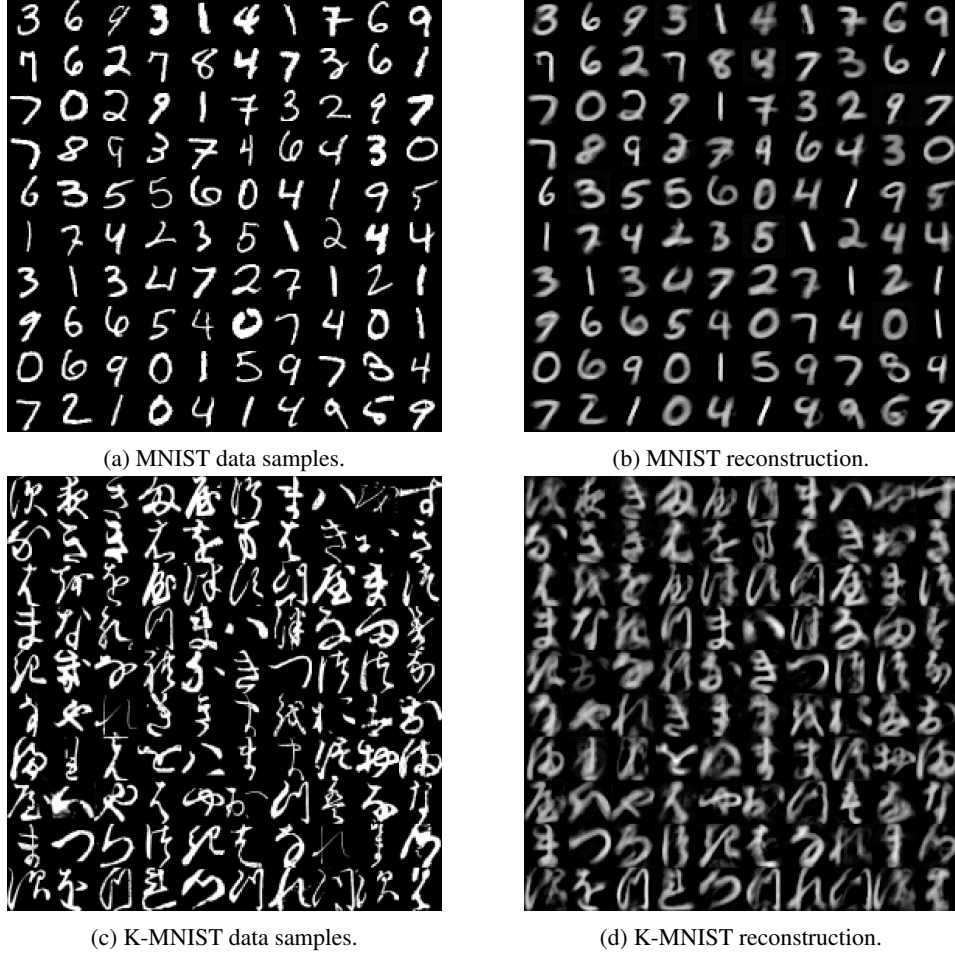


Figure 3: Reconstructions produced by the SNN when learned with ED-PFF. Left column (sub-figures a and c) present the randomly selected images from the target database while the right column (sub-figures b and d) present the reconstructed patterns produced by the recurrent spiking model. Top row presents results for MNIST while the bottom row presents results for K-MNIST.

where  $\mathbf{z}_\mu^0(t)$  is the activation trace of the output prediction spike vector  $\mathbf{s}_\mu^0(t)$  (produced by the local prediction of layer  $\ell = 0$  from layer  $\ell = 1$  - see Equation 13) at simulation step  $t$ .

Desirably, we see that the ED-FF model is able to produce reasonable reconstructions of the image patterns, demonstrating that it is enable to encode in its generative synapses information that is useful for decoding the very sparse spike train representations that its internal layers of LIF neurons produce. Note that the context  $\mathbf{y}$  was not clamped to our model when reconstruction ability was evaluated (which means that any contextual information that has been stored into the system’s synapses was used to determine how to reconstruct test samples).

### 3.3 Patch-Level Representations

We finally briefly investigate the representation capability of our spiking system in the context of image patches. Specifically, we extract patches of  $8 \times 8$  and  $12 \times 12$  pixels from a subset of the MNIST database (1000 image patterns, 10 from each class) and train a model with 2000 LIF units in both layers using the ED-FF procedure. The learned receptive fields, for each of the two patch settings, of the bottom-most layer of the trained model (i.e., layer  $\ell = 1$ ) are shown in Figure 4. Receptive fields in the bottom layer were extracted for visualization by randomly sampling, without replacement, 100 slices of the synaptic matrix  $\mathbf{W}^1$ . As observed in Figure 4, the receptive fields extract basic patterns at different resolutions; in the smaller  $8 \times 8$  patch model, we see simpler patterns emerge such as edges or stroke pieces (“strokelets”) of different orientations while in the larger  $12 \times 12$  patch model we observe portions of patterns that appear as “mini-templates” that could be used to compose larger digits.

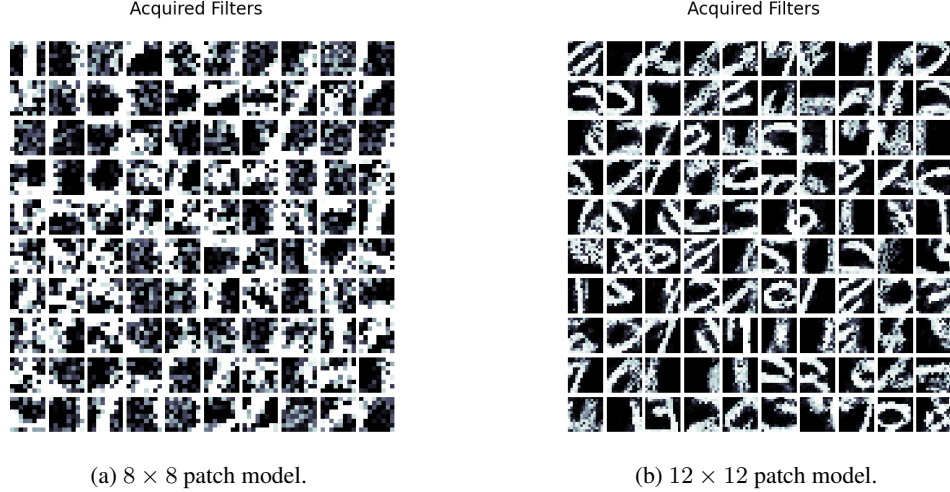


Figure 4: The receptive fields of 100 randomly chosen LIF neurons in the ED-FF model (in layer  $\ell = 1$ ), trained on patches. Shown are the receptive fields for: (Left) the  $8 \times 8$  patch model, and (Right) the  $12 \times 12$  patch model.

### 3.4 Discussion

**On Limitations:** Although our online contrastive forward-only credit assignment process for training recurrent spiking networks is promising, there are several limitations to consider. First, although the spiking model that we designed operates with bounded synaptic values (between  $-1, 1$ ), it does not operate with strictly positive values, which is an important hallmark of neurobiology (we cannot have negative synaptic efficacies). This is an unfortunate limitation that is made worse by the fact that the signs of the synaptic values could change throughout the course of simulated learning. Nevertheless, we remark that this issue could be potentially rectified by constraining all synapses to  $[0, 1]$  and then introducing an additional set of spiking inhibitory (or inter-inhibitory) neurons coupled to each layer that provide the inhibitory/depression signal that is offered by negative synaptic strengths. The proportion of inhibitory neurons to excitatory ones could further be desirably configured to furthermore adhere to Dale’s Law [73]. Future work will explore this possible reformulation, as the countering pressure offered by negative synapses is important for a goodness-based contrastive objective, much as the one employed by ED-FF, to work properly – ideally, inhibitory neurons should provide a similar type of pressure.

Beyond its use of synapses without a sign constraint, our current model does not include refractory periods, only implementing an instantaneous form of depolarization. However, this could be easily corrected by modifying Equation 3 to include an absolute refractory period much as has been done in [50]. Furthermore, the adaptive thresholds we presented in Equations 4, 16, and 22 are each calculated as a function of the total number of spikes across a layer  $\ell$  at time  $t$  whereas it would be more bio-physically realistic to have each LIF unit within a layer adapt its own specific scalar threshold.<sup>5</sup>

Finally, with respect to the event-driven forward-forward learning process itself, while we were able to desirably craft a simple update rule that operated at the spike-level (through a biologically plausible activation trace) there is still the drawback that the rule, much like its rated-coded sources of inspiration [25, 54], requires positive and negative data samples to compute synaptic adjustments. In this study, we exploited the fact that labels were readily available to serve as top-down context signals which made synthesizing negative samples easy – all we needed to do was simply select one of the incorrect class labels to create a negative context. However, in the interest of generalizing forward-forward based learning to a self-contained self-supervised framing, one would need to develop a mechanism for producing the negative samples based on the sensory input alone, without the aid of an explicit context. One way that this could possibly be done is through the use of the predictive/generative synapses of the ED-FF spike model to produce data confabulations that could serve as on-the-fly, dynamic negative patterns (much as was proposed in the rate-coded PFF algorithm [54]). However, the difficulty in synthesizing negative samples through the generative circuitry of our spiking model would be in crafting a process by which ancestral

<sup>5</sup>A per-neuron adaptive threshold could be modeled by another ordinary differential equation but we leave exploration of this to future work.

sampling could be efficiently conducted.<sup>6</sup> An alternative to synthesizing negative samples would be to design another neural circuit that produces context vector  $\mathbf{y}$  (both positive and negative variations) instead of using a provided label – a direction that is also more biologically realistic. Another drawback of using positive and negative samples in the kind of contrastive learning that we do in this work is that both types of data are used simultaneously. In [25, 54], it has been discussed that it will be important to examine alternative schemes for when negative samples are presented to and used by a neural system to adjust its synapses.

### 3.5 Related Work

Backprop has long faced criticism with respect to its neurobiological plausibility [10, 20, 70, 41, 21]. It is unlikely that backprop is a viable model of credit assignment in the brain. Among the biophysical issues [21, 41] that plague backprop, some of the key ones include: **1)** neural activities are explicitly stored to be used later for synaptic adjustment, **2)** error derivatives are backpropagated along a global feedback pathway [59] in order to generate useful teaching signals, **3)** the error signals move back along the same neural pathways used to forward propagate information (also known as the weight transport problem [21]), and, **4)** inference and learning are locked to be largely sequential [28] (instead of massively parallel as in the brain), and **5)** when processing temporal data, unfolding of the neural circuitry backward through time (i.e., backprop through time) is necessary before adjusting the synaptic weight values (which is clearly not the case for brain-like computation [55]).

Recently, there has been a growing interest in developing algorithms and computational models that attempt to circumvent or resolve some of the criticisms highlighted above. Among the most powerful and promising ones is predictive coding (PC) [24, 62, 18, 2, 65, 53], and among the most recent ones is forward-only learning, including approaches such as signal propagation [32, 31]), the forward-forward (FF) algorithm [25], and the predictive forward-forward (PFF) procedure [54]. These alternatives offer mechanisms for conducting credit assignment that is more consistent with elements of neurobiological learning while exhibiting performance similar to backprop.

Forward-only processes [32, 25, 54] have a unique advantage over other biological credit assignment schemes in that they only require forward propagation of information to facilitate learning, resulting in synaptic updates that are in the same spirit as Hebbian learning [23]. In addition, such processes are more suitable for on-chip learning (for neuromorphic hardware) given that they do not require distinct separate computational pathway(s) for transmitting teaching signals (which is required by backprop [64] and feedback alignment methods [37, 46]) or even error messages / error transmission pathways (which are required by predictive coding [62, 2, 53], representation alignment [58], and target propagation processes [36]). Desirably, this means that no specialized hardware is needed for computing activation function derivatives nor for maintaining and adjusting separate feedback transmission synapses that often require different adjustment rules [58, 55]. In addition, forward-only rules are generally faster than adaptation processes based on contrastive Hebbian learning [45, 26, 68], given that they do not require a negative phase computation to be conditioned on the statistics of a positive one (or vice versa). Finally, a forward-only scheme such as ED-FF naturally allows for incorporation of lateral competition within its layer-wise activities, offering corroborating evidence that cross-inhibitory activity patterns [78, 56] are important for neural computation (note that competitive learning has proven valuable when integrated with pure STDP-centric adaptation [71]).

## 4 Conclusion

In this work, we presented the event-driven forward-forward (ED-FF) process, a generalization of forward-forward and predictive forward-forward learning to the case of spike trains, for adjusting the synaptic efficacies of a recurrent spiking neural systems. Experimentally, we demonstrated that ED-FF adaptation could successfully learn discrete temporal representations that facilitated effective classification of image data as well as reconstruct the image inputs over time. Among the many potential directions that merit exploration with respect to ED-FF credit assignment, we believe that investigating how the adaptation process would operate in the context of far more complex data, such as natural images (assuming that the spiking system was equipped with the proper inductive biases) and sequences, e.g., video frames, will be important. Furthermore, it would be interesting to observe how spike-level circuitry, adapted via ED-FF learning, might be useful for neural-centric cognitive architectures [51, 52, 57], inspired by the success of models such as the Semantic Pointer Architecture (SPAUN) [74].

<sup>6</sup>Crafting an ancestral sampling process in the context of spike-trains is not nearly as clear as it is in the realm of rate-coded models in which predictive forward-forward learning was originally applied. Likely, one would need to develop a sampling scheme that is temporal in nature, which would likely be in of itself too expensive to run on-the-fly.

## Acknowledgements

We would like to thank Alexander Ororbia (Sr.) for useful feedback on the manuscript draft.

## References

- [1] AMODEI, D., AND HERNANDEZ, D. AI and compute. <https://openai.com/blog/ai-and-compute/>, May 2018.
- [2] BASTOS, A. M., USREY, W. M., ADAMS, R. A., MANGUN, G. R., FRIES, P., AND FRISTON, K. J. Canonical microcircuits for predictive coding. *Neuron* 76, 4 (2012), 695–711.
- [3] BI, G.-Q., AND POO, M.-M. Synaptic modifications in cultured hippocampal neurons: dependence on spike timing, synaptic strength, and postsynaptic cell type. *Journal of neuroscience* 18, 24 (1998), 10464–10472.
- [4] BREVINI, B. Black boxes, not green: Mythologizing artificial intelligence and omitting the environment. *Big Data & Society* 7, 2 (2020), 2053951720935141.
- [5] BUBECK, S., CHANDRASEKARAN, V., ELDAN, R., GEHRKE, J., HORVITZ, E., KAMAR, E., LEE, P., LEE, Y. T., LI, Y., LUNDBERG, S., ET AL. Sparks of artificial general intelligence: Early experiments with gpt-4. *arXiv preprint arXiv:2303.12712* (2023).
- [6] CAULFIELD, H. J., KINSER, J., AND ROGERS, S. K. Optical neural networks. *Proceedings of the IEEE* 77, 10 (1989), 1573–1583.
- [7] CLANUWAT, T., BOBER-IRIZAR, M., KITAMOTO, A., LAMB, A., YAMAMOTO, K., AND HA, D. Deep learning for classical japanese literature, 2018.
- [8] CLARK, A. *Surfing uncertainty: Prediction, action, and the embodied mind*. Oxford University Press, 2015.
- [9] COVI, E., DONATI, E., LIANG, X., KAPPEL, D., HEIDARI, H., PAYVAND, M., AND WANG, W. Adaptive extreme edge computing for wearable devices. *Frontiers in Neuroscience* 15 (2021), 611300.
- [10] CRICK, F. The recent excitement about neural networks. *Nature* 337, 6203 (1989), 129–132.
- [11] DEVLIN, J., CHANG, M.-W., LEE, K., AND TOUTANOVA, K. Bert: Pre-training of deep bidirectional transformers for language understanding. *arXiv preprint arXiv:1810.04805* (2018).
- [12] DIEHL, P. U., AND COOK, M. Unsupervised learning of digit recognition using spike-timing-dependent plasticity. *Frontiers in computational neuroscience* 9 (2015), 99.
- [13] DUVILLIER, J., KILLINGER, M., HEGGARTY, K., YAO, K., ET AL. All-optical implementation of a self-organizing map: a preliminary approach. *Applied optics* 33, 2 (1994), 258–266.
- [14] ELIASMITH, C., AND ANDERSON, C. H. *Neural engineering: Computation, representation, and dynamics in neurobiological systems*. MIT press, 2004.
- [15] ELIASMITH, C., STEWART, T. C., CHOO, X., BEKOLAY, T., DEWOLF, T., TANG, Y., AND RASMUSSEN, D. A large-scale model of the functioning brain. *science* 338, 6111 (2012), 1202–1205.
- [16] FLORIDI, L., AND CHIRIATTI, M. Gpt-3: Its nature, scope, limits, and consequences. *Minds and Machines* 30, 4 (2020), 681–694.
- [17] FRENKEL, C., LEFEBVRE, M., AND BOL, D. Learning without feedback: Direct random target projection as a feedback-alignment algorithm with layerwise feedforward training. *arXiv preprint arXiv:1909.01311* (2019).
- [18] FRISTON, K. The free-energy principle: a unified brain theory? *Nature reviews neuroscience* 11, 2 (2010), 127–138.
- [19] FURBER, S. Large-scale neuromorphic computing systems. *Journal of neural engineering* 13, 5 (2016), 051001.
- [20] GARDNER, D. *The Neurobiology of neural networks*. MIT Press, 1993.
- [21] GROSSBERG, S. Competitive learning: From interactive activation to adaptive resonance. *Cognitive science* 11, 1 (1987), 23–63.
- [22] HAZAN, H., SAUNDERS, D., SANGHAVI, D. T., SIEGELMANN, H., AND KOZMA, R. Unsupervised learning with self-organizing spiking neural networks. In *2018 International Joint Conference on Neural Networks (IJCNN)* (2018), IEEE, pp. 1–6.
- [23] HEBB, DONALD O, E. A. The organization of behavior, 1949.
- [24] HELMHOLTZ, H. v. Treatise on physiological optics, 3 vols. *Treatise* (1924).

- [25] HINTON, G. The forward-forward algorithm: Some preliminary investigations. *arXiv preprint arXiv:2212.13345* (2022).
- [26] HINTON, G. E. Training products of experts by minimizing contrastive divergence. *Neural computation* 14, 8 (2002), 1771–1800.
- [27] ITOH, M., AND CHUA, L. O. Memristor oscillators. *International journal of bifurcation and chaos* 18, 11 (2008), 3183–3206.
- [28] JADERBERG, M., CZARNECKI, W. M., OSINDERO, S., VINYALS, O., GRAVES, A., AND KAVUKCUOGLU, K. Decoupled neural interfaces using synthetic gradients. *arXiv preprint arXiv:1608.05343* (2016).
- [29] JADERBERG, M., CZARNECKI, W. M., OSINDERO, S., VINYALS, O., GRAVES, A., SILVER, D., AND KAVUKCUOGLU, K. Decoupled neural interfaces using synthetic gradients. In *International conference on machine learning* (2017), PMLR, pp. 1627–1635.
- [30] KINGMA, D., AND BA, J. Adam: A method for stochastic optimization. *arXiv preprint arXiv:1412.6980* (2014).
- [31] KOHAN, A., RIETMAN, E. A., AND SIEGELMANN, H. T. Signal propagation: The framework for learning and inference in a forward pass. *IEEE Transactions on Neural Networks and Learning Systems* (2023).
- [32] KOHAN, A. A., RIETMAN, E. A., AND SIEGELMANN, H. T. Error forward-propagation: Reusing feedforward connections to propagate errors in deep learning. *arXiv preprint arXiv:1808.03357* (2018).
- [33] KRESTINSKAYA, O., JAMES, A. P., AND CHUA, L. O. Neuromemristive circuits for edge computing: A review. *IEEE transactions on neural networks and learning systems* 31, 1 (2019), 4–23.
- [34] KUON, I., TESSIER, R., ROSE, J., ET AL. Fpga architecture: Survey and challenges. *Foundations and Trends® in Electronic Design Automation* 2, 2 (2008), 135–253.
- [35] LECUN, Y. The mnist database of handwritten digits. <http://yann.lecun.com/exdb/mnist/> (1998).
- [36] LEE, D.-H., ZHANG, S., FISCHER, A., AND BENGIO, Y. Difference target propagation. In *Joint European Conference on Machine Learning and Knowledge Discovery in Databases* (2015), Springer, pp. 498–515.
- [37] LILLICRAP, T. P., COWNDEN, D., TWEED, D. B., AND AKERMAN, C. J. Random feedback weights support learning in deep neural networks. *arXiv preprint arXiv:1411.0247* (2014).
- [38] MAASS, W. Networks of spiking neurons: the third generation of neural network models. *Neural networks* 10, 9 (1997), 1659–1671.
- [39] MAASS, W. Computation with spiking neurons. *The handbook of brain theory and neural networks* (2003), 1080–1083.
- [40] MAASS, W., AND BISHOP, C. M. *Pulsed neural networks*. MIT press, 2001.
- [41] MARBLESTONE, A. H., WAYNE, G., AND KORDING, K. P. Toward an integration of deep learning and neuroscience. *Frontiers in computational neuroscience* (2016), 94.
- [42] MEROLLA, P., ARTHUR, J., AKOPYAN, F., IMAM, N., MANOHAR, R., AND MODHA, D. S. A digital neurosynaptic core using embedded crossbar memory with 45pj per spike in 45nm. In *2011 IEEE custom integrated circuits conference (CICC)* (2011), IEEE, pp. 1–4.
- [43] MOHEMMED, A., SCHLIEBS, S., MATSUDA, S., AND KASABOV, N. Span: Spike pattern association neuron for learning spatio-temporal spike patterns. *International journal of neural systems* 22, 04 (2012), 1250012.
- [44] MOSTAFA, H., RAMESH, V., AND CAUWENBERGHS, G. Deep supervised learning using local errors. *Frontiers in neuroscience* 12 (2018), 608.
- [45] MOVELLAN, J. R. Contrastive hebbian learning in the continuous hopfield model. In *Connectionist models*. Elsevier, 1991, pp. 10–17.
- [46] NØKLAND, A. Direct feedback alignment provides learning in deep neural networks. In *Advances in Neural Information Processing Systems* (2016), pp. 1037–1045.
- [47] OMONDI, A. R., AND RAJAPAKSE, J. C. *FPGA implementations of neural networks*, vol. 365. Springer, 2006.
- [48] O’REILLY, R. C. Biologically plausible error-driven learning using local activation differences: The generalized recirculation algorithm. *Neural computation* 8, 5 (1996), 895–938.
- [49] O’REILLY, R. C., AND MUNAKATA, Y. *Computational explorations in cognitive neuroscience: Understanding the mind by simulating the brain*. MIT press, 2000.

- [50] ORORBIA, A. Spiking neural predictive coding for continual learning from data streams. *arXiv preprint arXiv:1908.08655* (2019).
- [51] ORORBIA, A., AND KELLY, M. A. Towards a predictive processing implementation of the common model of cognition. *arXiv preprint arXiv:2105.07308* (2021).
- [52] ORORBIA, A., AND KELLY, M. A. Cogngen: Building the kernel for a hyperdimensional predictive processing cognitive architecture. In *Proceedings of the Annual Meeting of the Cognitive Science Society* (2022), vol. 44.
- [53] ORORBIA, A., AND KIFER, D. The neural coding framework for learning generative models. *Nature communications* 13, 1 (2022), 1–14.
- [54] ORORBIA, A., AND MALI, A. The predictive forward-forward algorithm. *arXiv preprint arXiv:2301.01452* (2022).
- [55] ORORBIA, A., MALI, A., GILES, C. L., AND KIFER, D. Continual learning of recurrent neural architectures by locally aligning distributed representations. *arXiv preprint arXiv:1810.07411* (2018).
- [56] ORORBIA, A. G. Continual competitive memory: A neural system for online task-free lifelong learning. *arXiv preprint arXiv:2106.13300* (2021).
- [57] ORORBIA, A. G., AND KELLY, M. A. Maze learning using a hyperdimensional predictive processing cognitive architecture. In *Artificial General Intelligence: 15th International Conference, AGI 2022, Seattle, WA, USA, August 19–22, 2022, Proceedings* (2023), Springer, pp. 321–331.
- [58] ORORBIA, A. G., AND MALI, A. Biologically motivated algorithms for propagating local target representations. In *Proceedings of the AAAI Conference on Artificial Intelligence* (2019), vol. 33, pp. 4651–4658.
- [59] ORORBIA, A. G., AND MALI, A. Biologically motivated algorithms for propagating local target representations. In *Proceedings of the AAAI Conference on Artificial Intelligence* (2019), vol. 33, pp. 4651–4658.
- [60] ORORBIA II, A. G., HAFFNER, P., REITTER, D., AND GILES, C. L. Learning to adapt by minimizing discrepancy. *arXiv preprint arXiv:1711.11542* (2017).
- [61] PATTERSON, D., GONZALEZ, J., LE, Q., LIANG, C., MUNGUIA, L.-M., ROTHCHILD, D., SO, D., TEXIER, M., AND DEAN, J. Carbon emissions and large neural network training. *arXiv preprint arXiv:2104.10350* (2021).
- [62] RAO, R. P., AND BALLARD, D. H. Predictive coding in the visual cortex: a functional interpretation of some extra-classical receptive-field effects. *Nature neuroscience* 2, 1 (1999).
- [63] ROY, K., JAISWAL, A., AND PANDA, P. Towards spike-based machine intelligence with neuromorphic computing. *Nature* 575, 7784 (2019), 607–617.
- [64] RUMELHART, D. E., HINTON, G. E., AND WILLIAMS, R. J. Learning representations by back-propagating errors. *nature* 323, 6088 (1986), 533–536.
- [65] SALVATORI, T., SONG, Y., HONG, Y., SHA, L., FRIEDER, S., XU, Z., BOGACZ, R., AND LUKASIEWICZ, T. Associative memories via predictive coding. *Advances in Neural Information Processing Systems* 34 (2021), 3874–3886.
- [66] SALVATORI, T., SONG, Y., XU, Z., LUKASIEWICZ, T., BOGACZ, R., LIN, H., FAN, Y., ZHANG, J., BAI, B., AND XU, ZHENGHUA, E. A. Reverse differentiation via predictive coding. In *Proceedings of the 36th AAAI Conference on Artificial Intelligence , AAAI 2022 , Vancouver, BC, Canada, February 22–March 1 , 2022* (2022), vol. 10177, AAAI Press, pp. 507–524.
- [67] SAMADI, A., LILICRAP, T. P., AND TWEED, D. B. Deep learning with dynamic spiking neurons and fixed feedback weights. *Neural computation* 29, 3 (2017), 578–602.
- [68] SCELLIER, B., AND BENGIO, Y. Equilibrium propagation: Bridging the gap between energy-based models and backpropagation. *Frontiers in computational neuroscience* 11 (2017), 24.
- [69] SCHWARTZ, R., DODGE, J., SMITH, N. A., AND ETZIONI, O. Green AI. *Communications of the ACM* 63, 12 (2020), 54–63.
- [70] SHEPHERD, G. M. The significance of real neuron architectures for neural network simulations. *Computational neuroscience* (1990), 82–96.
- [71] SONG, S., MILLER, K. D., AND ABBOTT, L. F. Competitive hebbian learning through spike-timing-dependent synaptic plasticity. *Nature neuroscience* 3, 9 (2000), 919–926.
- [72] SPRATLING, M. W. A hierarchical predictive coding model of object recognition in natural images. *Cognitive computation* 9, 2 (2017), 151–167.

- [73] SPREKELER, H. Functional consequences of inhibitory plasticity: homeostasis, the excitation-inhibition balance and beyond. *Current opinion in neurobiology* 43 (2017), 198–203.
- [74] STEWART, T., CHOO, F.-X., AND ELIASMITH, C. Spaun: A perception-cognition-action model using spiking neurons. In *Proceedings of the Annual Meeting of the Cognitive Science Society* (2012), vol. 34.
- [75] STRUBELL, E., GANESH, A., AND MCCALLUM, A. Energy and policy considerations for deep learning in NLP. In *Proceedings of the 57th Annual Meeting of the Association for Computational Linguistics* (Florence, Italy, July 2019), Association for Computational Linguistics, pp. 3645–3650.
- [76] THOMAS, A. Memristor-based neural networks. *Journal of Physics D: Applied Physics* 46, 9 (2013), 093001.
- [77] VAN DER MAATEN, L., AND HINTON, G. Visualizing data using t-sne. *Journal of machine learning research* 9, 11 (2008).
- [78] WHITE, R. H. Competitive hebbian learning. In *IJCNN-91-Seattle International Joint Conference on Neural Networks* (1991), vol. 2, IEEE, pp. 949–vol.
- [79] YIN, S., VENKATARAMANAIAH, S. K., CHEN, G. K., KRISHNAMURTHY, R., CAO, Y., CHAKRABARTI, C., AND SEO, J.-S. Algorithm and hardware design of discrete-time spiking neural networks based on back propagation with binary activations. In *2017 IEEE Biomedical Circuits and Systems Conference (BioCAS)* (2017), IEEE, pp. 1–5.
- [80] ZHAO, G., WANG, T., LI, Y., JIN, Y., LANG, C., AND LING, H. The cascaded forward algorithm for neural network training. *arXiv preprint arXiv:2303.09728* (2023).